Available online at www.sciencedirect.com

SciVerse ScienceDirect

Ceramics International 39 (2013) 2231–2237

CERAMICS INTERNATIONAL

www.elsevier.com/locate/ceramint

Microstructure and electrical properties of rare earth doped ZnO-based varistor ceramics

Ji-le Li, Guo-hua Chen*, Chang-lai Yuan

School of Materials Science and Engineering, Guilin University of Electronic Technology, Guilin 541004, China

Received 8 August 2012; accepted 23 August 2012
Available online 4 September 2012

Abstract

ZnO-based varistor ceramics doped with Nd_2O_3 and Y_2O_3 have been prepared by the conventional ceramics method. The phase composition, microstructure and electrical properties of the ceramics have been investigated by XRD, SEM and a *V–I* source/measure unit. The XRD and EDS analyses show the presence of ZnO, Bi_2O_3, $Zn_7Sb_2O_{12}$, Y_2O_3, Nd-rich phase and Y-containing Bi-rich phase. The electrical properties analyzed show that the nonlinear coefficient of the varistor ceramics is in the range of 4.4–70.2, the threshold voltage is in the range of 247.1–1288.8 V/mm, and the leakage current is in the range of 1.51–214.6 μA/cm^2. The 0.25 mol% Nd_2O_3 added varistor ceramics with 0.10 mol% Y_2O_3 sintered at 1050 °C exhibits excellent electrical properties with the high threshold voltage of 556.4 V/mm, the nonlinear coefficient of 61 and the leakage current of 1.55 μA/cm^2. The results illustrate that doping Nd_2O_3 and Y_2O_3 in ZnO-based varistor ceramics may be a very promising route for the production of the higher threshold voltage and the nonlinear coefficient of ZnO-based varistor ceramics.

Keywords: E. Varistors; ZnO-based ceramics; Rare earth; Microstructure

1. Introduction

ZnO varistors are semiconducting ceramics fabricated by sintering of ZnO powders with small amounts of additives such as Bi_2O_3, CoO, MnO, and Sb_2O_3 and so on to further enhance the non-linearity of the varistor's behavior [1]. The highly nonlinear electric field–current density (*E–J*) and a high energy absorption capability characteristic of ZnO varistors are widely used as surge absorbers in electronic circuits, devices and electrical power systems to protect against dangerous over-voltage surges. The non-linear current–voltage characteristics of ZnO varistor ceramics is attributed to the existence of a double Schottky barrier at the electrically active grain boundary layer, which is essentially formed by segregation of large ionic varistor forming oxides. These Schottky barriers arise from the trapping of electrons and control the electrical characteristics of varistors [2,3].

As the non-linear electrical behavior occurs at the boundary of each semiconducting ZnO grain, the varistor can be defined as a multi-junction device composed of series and parallel connections of grain boundaries in which each has a breakdown voltage of 3 V. Thus, to achieve a given breakdown voltage, one can change the varistor thickness or one can vary the grain size to increase the number of barriers or grain boundaries [4]. High-voltage varistor ceramics require a fine-grained microstructure and Sb_2O_3 is usually added to inhibit the ZnO grain growth. More recently, high breakdown voltage varistors is the technical trend in arrester field since it can be reduce element size and weight [5]. It is well known that rare earth elements can improve electric field of ZnO-based varistor ceramics and show similar effects to Bi_2O_3 which makes potential barriers at the grain boundaries by becoming itself a layer of inter-granular material and by supplying ions to the ZnO grain boundaries [1]. Most of the studies [2,5–7] on ZnO (or ZnO–Bi_2O_3) based and Pr_6O_{11} based [8–11] varistor ceramics doped with rare earth oxides have been made in order to understand the influence of different rare earth oxides (such as Sm_2O_3,

*Corresponding author. Tel.: +86 7732291434; fax: +86 7732290129.
E-mail addresses: cgh1682002@163.com, chengh@guet.edu.cn (G.-H. Chen).

0272-8842/$ - see front matter © 2012 Elsevier Ltd and Techna Group S.r.l. All rights reserved.
http://dx.doi.org/10.1016/j.ceramint.2012.08.067

Er_2O_3, Sc_2O_3,Y_2O_3, Nd_2O_3 and La_2O_3) on the microstructure and electrical properties of the ZnO varistor ceramics. These investigations indicate that rare earth oxides may play an important role in controlling different operation parameters of these kinds of varistors devices. Namh et al. [11] and Wang et al. [12] reported that the addition of Nd_2O_3 to the ZnO-based varistors can greatly enhance the nonlinearity of the varistor's behavior. However, the varistors that have a high nonlinearity exhibit very poor in breakdown field. The breakdown field decreases with the increase of Nd_2O_3 content when the content of Nd_2O_3 is ≥ 0.04 mol% [13]. Bernik et al. [7,14] found that the fine-grained Y_2O_3-containing phase present at the grain boundaries strongly inhibits ZnO grain growth while the leakage current (J_L) increases with increasing amounts of Y_2O_3. To overcome a few flaws of not only poor breakdown field of Nd_2O_3-doped-ZnO-based varistors but also the large leakage current of Y_2O_3-doped-ZnO-based varistors. It is necessary to investigate the effect of incorporation of novel mixed rare earths Nd_2O_3 and Y_2O_3 on microstructure and electrical properties of ZnO-based varistors.

Our previous studies have confirmed that the optimum content of only doping Nd_2O_3 is about 0.25 mol% in the ZnO-based varistor ceramics. In this work, the aim is to investigate the effect of incorporation of Nd_2O_3 (0.25 mol%) and various Y_2O_3 contents on microstructure and electrical properties of ZnO-based varistor ceramics. The relation between the electrical characteristics of ZnO-based varistor ceramics and rare earth content has also been investigated.

2. Experimental procedure

2.2. Sample preparation

ZnO-based varistor samples with the nominal composition shown in Table 1 were prepared by the traditional ceramics method. Raw materials were mixed by ball-milling with zirconia balls and alcohol in a polypropylene bottle for 24 h and the mixture was dried at about 70 °C for 12 h followed by calcinations at 750 °C for 2 h. The calcined mixture was remilled in alcohol medium for 24 h. After drying, mixing with 4 wt% polyvinyl alcohol (PVA) solution, the granulated powders were pressed uniaxially into discs of 18 mm in diameter and 1.3 mm in thickness at a pressure of 80 MPa. The pressed discs were then fired at 600 °C for 1 h to expel the binder before sintering at temperatures in the range of 1050–1150 °C for 2 h in air with heating and cooling rates of 4 °C/min in air. The resulting dark-green ceramic bodies were approximately 14 mm in diameter and 1.1 mm in thickness. Silver paste was coated on both faces of samples and the silver electrodes were formed by heating at 600 °C for 10 min. The diameter of electrodes was 12 mm.

2.2. Microstructure examination

The surfaces of the sintered samples were observed by a scanning electron microscope (SEM, Model JSM-5610LV, JEOL, Japan) equipped with energy dispersive X-ray spectroscopy (EDS). The average ZnO grain size (D) was determined from SEM images. The compositional analysis of the selected areas was determined by an attached energy dispersion X-ray spectroscope (EDS) system. The phase composition and crystallinity of the sintered ceramics were determined using an X-ray diffractometer (XRD) ($Cu_{K\alpha}$, $\lambda = 1.54059$ Å, Model D8-Advance, Bruker, Germany).The bulk density of the samples was measured using the Archimedes method [15].

2.3. Electrical property measurement

The DC electrical measurements at room temperature were measured using a V–I measure unit (Model CJ1001, Changzhou Chuangjie Lightning Protection Co., Ltd., China). The current was recorded by increasing the applied voltage step by step manually to characterize the electric field–current density (E–J) behavior of different ZnO-based varistor ceramics. The nominal varistor voltages (V_N) at 1.0 mA was measured and the threshold voltage $E_{1\ mA}$ (V/mm) ($E_{1\ mA} = V_N$ (1 mA)/H; H is the thickness of the sample in mm). The leakage current (I_L) was measured at $0.75V_N$ (1 mA), the leakage current density (J_L) was calculated by $J_L = I_L/S$, where S is the silver electrode area. The nonlinear coefficient α was obtained from the equation: $\alpha = 1/\lg(V_{1\ mA}/V_{0.1\ mA})$, the $V_{1\ mA}$ and $V_{0.1\ mA}$ are the

Table1
Composition of Nd_2O_3 and Y_2O_3 co-doped ZnO-based varistor ceramics.

Sample	Composition (mol%)							
	ZnO	Bi_2O_3	Co_2O_3	MnO_2	Sb_2O_3	Cr_2O_3	Nd_2O_3	Y_2O_3
A0	96.30	0.7	1.0	0.5	1.0	0.5	0	0
A1	96.05	0.7	1.0	0.5	1.0	0.5	0.25	0
A2	95.95	0.7	1.0	0.5	1.0	0.5	0.25	0.1
A3	95.91	0.7	1.0	0.5	1.0	0.5	0.25	0.14
A4	95.75	0.7	1.0	0.5	1.0	0.5	0.25	0.30
A5	95.55	0.7	1.0	0.5	1.0	0.5	0.25	0.50

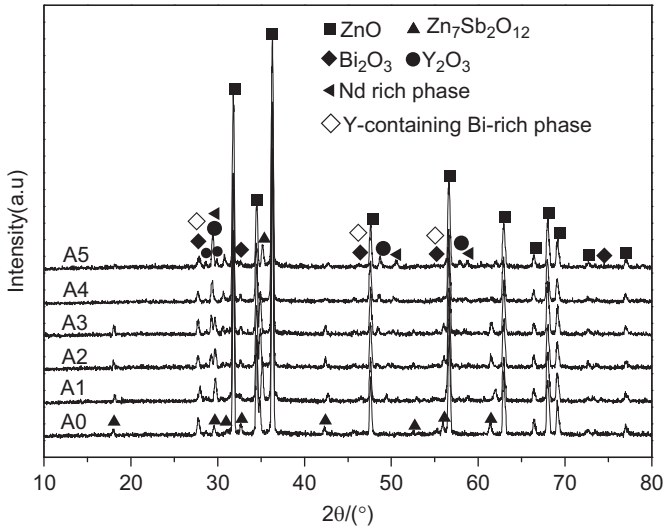

Fig. 1. XRD patterns of rare earth doped ZnO varistor ceramics sintered at 1100 °C for 2 h.

electric voltages corresponding to 1.0 mA and 0.1 mA, respectively.

3. Results and discussion

The XRD patterns of the ZnO-based varistor ceramics doped with Nd_2O_3 and various Y_2O_3 sintered at 1100 °C for 2 h are shown in Fig. 1. The XRD patterns reveal the presence of primary phase ZnO and Bi_2O_3, $Zn_7Sb_2O_{12}$, Y_2O_3, Nd-rich phase and Y-containing Bi-rich phase as minor secondary phases. As the Y_2O_3 content increases in the samples, additional peaks are evident due to the formation of Y_2O_3 phase in the varistor ceramics. At the same time, some of the peaks corresponding to spinel phase of $Zn_7Sb_2O_{12}$ diminish with higher content of rare earth.

Fig. 2 shows the SEM micrographs of ZnO-based varistor ceramics with Nd_2O_3 and various Y_2O_3 contents

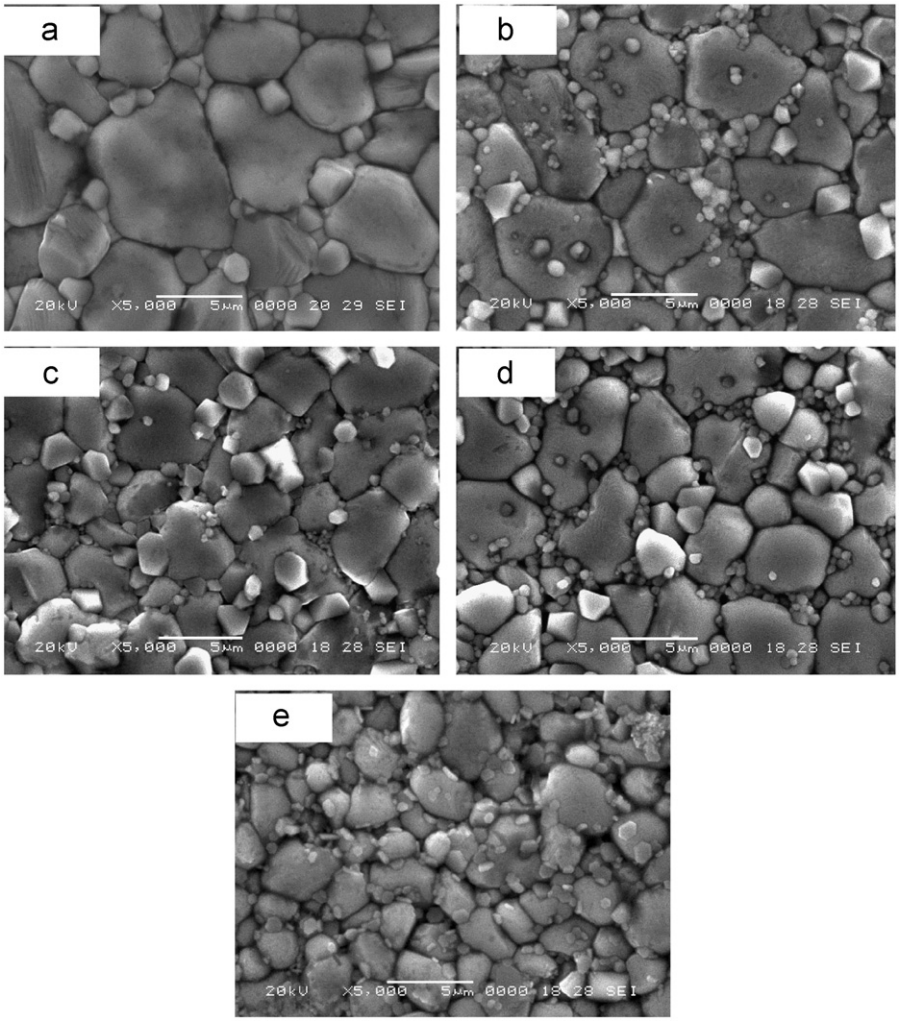

Fig. 2. SEM images of rare earth doped ZnO varistor ceramics sintered at 1100 °C for 2 h: (a) A1, (b) A2, (c) A3, (d) A4 and (e) A5.

sintered at 1100 °C for 2 h. The microstructure consists of ZnO grain as a primary phase and an inter-granular layer as a secondary phase. It can be observed the average grain size decreases from 6.19 to 3.18 μm with increasing Y_2O_3 content shown in Fig. 2a–e. As the Y_2O_3 content increases, the crystallite sizes of the secondary phases including Nd-rich phase, Y_2O_3 phase and Y-containing Bi-rich phase become smaller and the quantities increase dramatically. The inter-granular phase gradually more distributes at the grain boundaries and particularly the nodal points, which might be due to formation of smaller grain size of ZnO in these samples. The appearance of these XRD peaks may also indicate the development of Nd-rich phase and Y-containing Bi-rich phase in the form of Zn–Bi–Sb–Cr–Co–Y–Nd–O as observed in EDS [8]. As shown in the EDS analysis in Fig. 3, no Nd peak and Y peak can be found in the ZnO grain within the EDS detection limit. It is believed that this is attributed to the segregation of Nd and Y toward grain boundaries due to the difference of ionic radius. The Nd-rich phase and Y-containing Bi-rich phase act as a growth moderator for ZnO grain at the grain boundaries and hinder ion transfer.

Fig. 4 shows the relative density of the 0.25 mol% Nd_2O_3 added-ZnO based varistor as a function of Y_2O_3 content sintered at different temperatures for 2 h. The results show that the higher the sintering temperature is, the lower the density of the varistor ceramics is. This is related with the vaporization of Bi_2O_3 from the ZnO-based varistor ceramics. The melting point of Bi_2O_3 is 825 °C, which decreases to 750 °C when coexisting with ZnO [1]. Hence, a liquid phase is formed when sintered at 1050–1150 °C. Generally, the varistor ceramics sintered at 1050 °C have the maximum density. The higher the sintering temperature is, the more the Bi_2O_3 volatilizes. Hence, the densification that occurs during sintering depends on the Bi_2O_3 vaporization [16]. It is noted that the relative densities almost increase with Y_2O_3 content when Y_2O_3 content is ≤ 0.14 mol%. It is well known that atomic weight of Zn (65.39 g) is less than the atomic weight of Y (88.91 g), and Y^{3+} ion has a larger radius (0.093 nm) than that of Zn^{2+} ion (0.074 nm). Thus, initial additions of Y_2O_3 mainly change grain size and phase distribution [17,18]. The initial increase in densification may be due to great atomic weight of Y element. However, the decrease

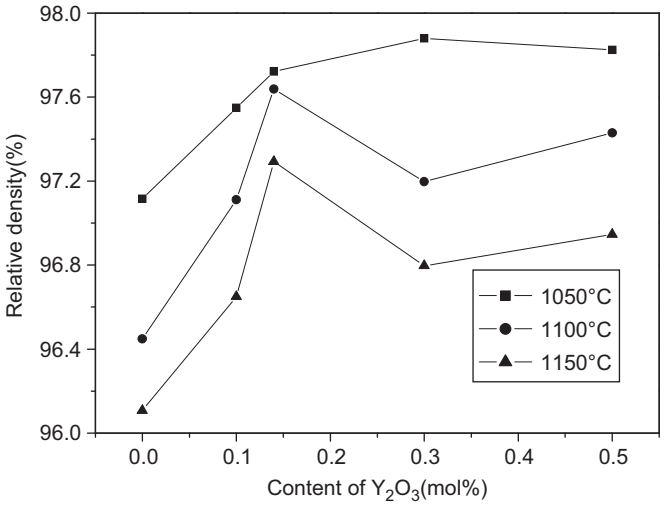

Fig. 4. Relative density of the 0.25 mol% Nd_2O_3 added ZnO based varistor as a function of Y_2O_3 content sintered at different temperatures.

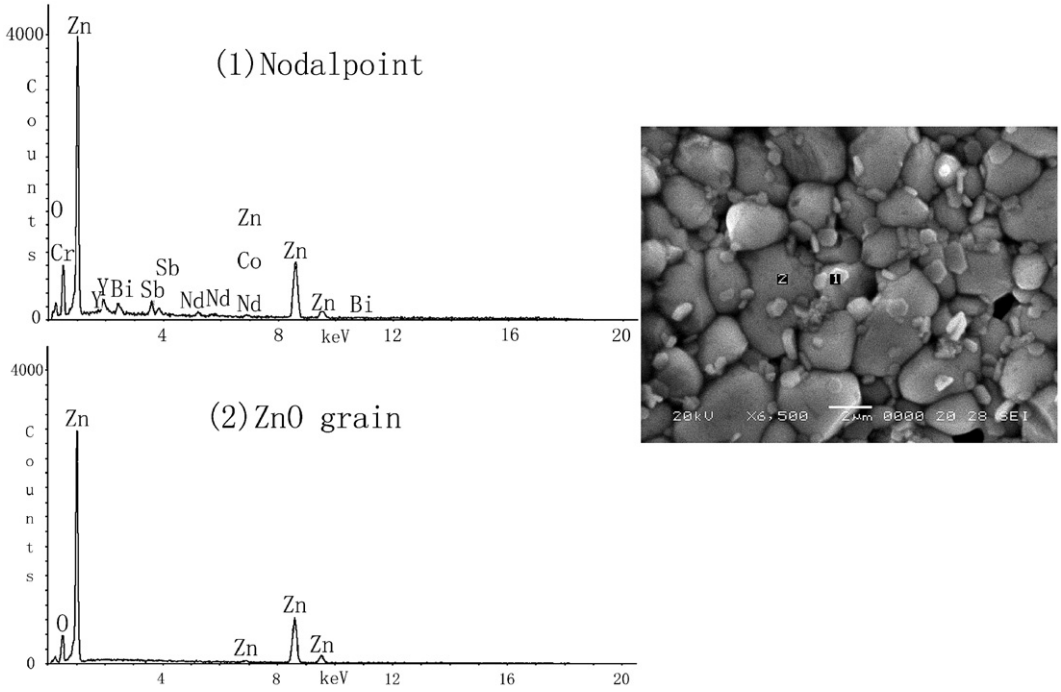

Fig. 3. EDS analyses of marked points of ZnO-based varistor ceramics doped with 0.25 mol% Nd_2O_3 and 0.5 mol% Y_2O_3: (1) nodal point and (2) ZnO grain.

in the relative density of the varistor ceramics with higher Y_2O_3 content may be due to the increase of inter-granular porosity resulting from fine grain size [19].

Fig. 5 shows the electric field–current density (*E–J*) characteristics of the ZnO-based varistor ceramics for different contents of Nd_2O_3 and Y_2O_3 sintered at different temperatures. The varistor properties are characterized by non-ohmicity in the *E–J* characteristics. It is observed that the J_L for all the varistor samples increases slowly below a breakdown/threshold voltage and above this electric field there is a sudden rise in J_L. It is clearly shown that the conduction characteristics can be divided into two regions, which are of very high impedance in pre-breakdown at low field and very low impedance in breakdown at high field. The sharper the knee of the curves between the two regions is, the better the nonlinear property is [20]. The un-doped rare earth sample (A0) showed very poor non-ohmic properties. On adding 0.25 mol% Nd_2O_3 and proper amounts of Y_2O_3, the knee gradually becomes more

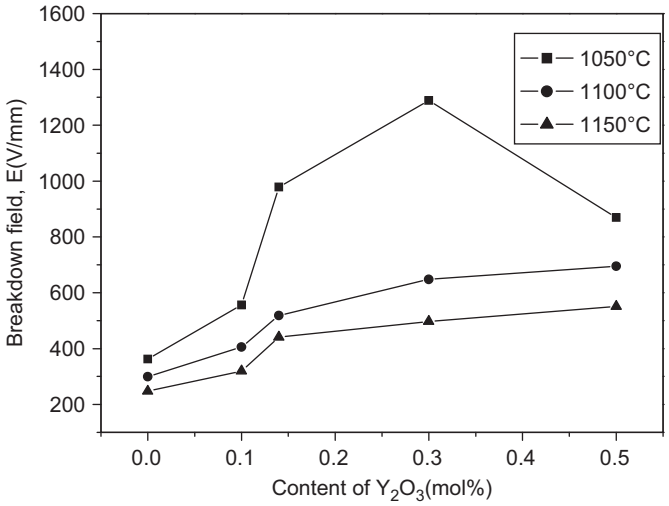

Fig. 6. Breakdown field (*E*) of the 0.25 mol% Nd_2O_3 added-ZnO based varistor as a function of Y_2O_3 content sintered at different temperatures.

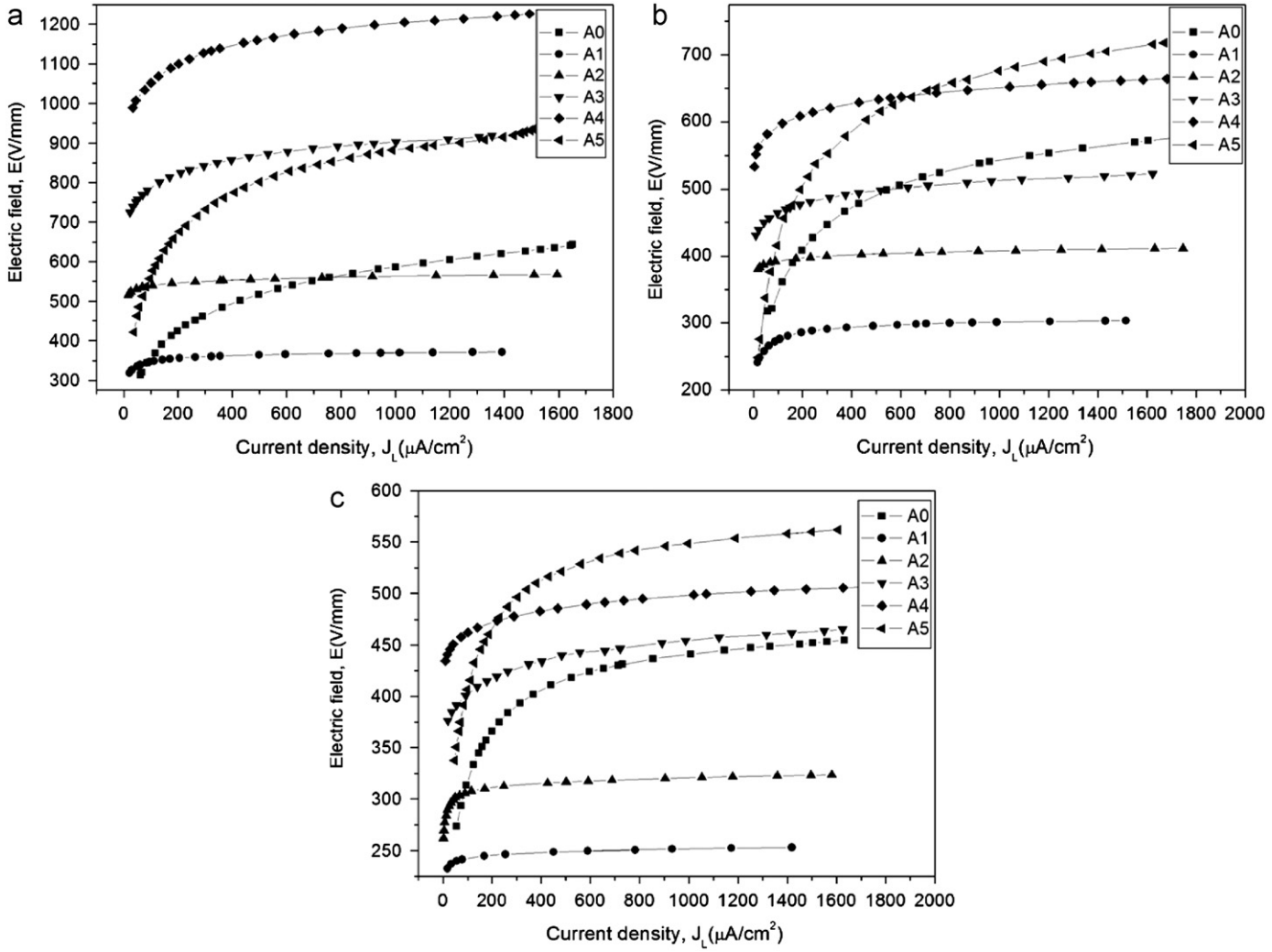

Fig. 5. Electric field to current density (*E–J*) curves of rare earth co-doped ZnO-based varistor ceramics sintered at different temperatures. (a) 1050 °C, (b) 1100 °C and (c) 1150 °C.

pronounced. Therefore, the incorporation of Nd_2O_3 and Y_2O_3 seems to remarkably enhance varistor properties. It is noticed that the *E–J* curve of the ceramic sample doped with 0.25 mol% Nd_2O_3 and 0.10 mol% Y_2O_3 has good varistor properties and low current density values.

Fig. 6 shows the variation of the threshold voltage of the 0.25 mol% Nd_2O_3 added ZnO-based varistor ceramics as a function of Y_2O_3 content sintered at different temperatures. When the sintering temperature is fixed, the threshold voltage increases with the increase of Y_2O_3 content except at 1050 °C. The minimum value of the threshold voltage is 247.1 V/mm for un-doped sample A0 sintered at 1150 °C, and the maximum threshold voltage of 1288.8 V/mm can be obtained for the 0.3 mol% Y_2O_3 doped sample A3 sintered at 1050 °C. The stabilizing effect of segregated Y^{3+} cations on ZnO grain can inhibit the growth of ZnO grains, resulting in smaller grain size. Therefore, the fine crystalline microstructure of the ZnO-based ceramics can improve the threshold voltage. It is observed that the breakdown voltage decreases with the increase of the sintering temperature for the same samples, which is attributed to the decrease in the number of grain boundaries caused by the increase of the ZnO grain size. This is very effective for high voltage varistor with a compact size.

Fig. 7 illustrates the variation of the nonlinear coefficient with various contents of Y_2O_3 in the 0.25 mol% Nd_2O_3 doped-ZnO based varistor ceramics sintered at different temperatures. It is found that only Nd_2O_3 doped-ZnO based varistor ceramics show high nonlinear coefficient, which is well in agreement with the report by Namh et al. [11] and Wang et al. [12]. It can be seen that the nonlinear coefficient initially increases and then decreases with the increase of Y_2O_3 content. The nonlinear coefficient varies from a maximum value of 70.2 to a minimum value of 4.8 in the ZnO-based varistor ceramics sintered at 1100 °C. The

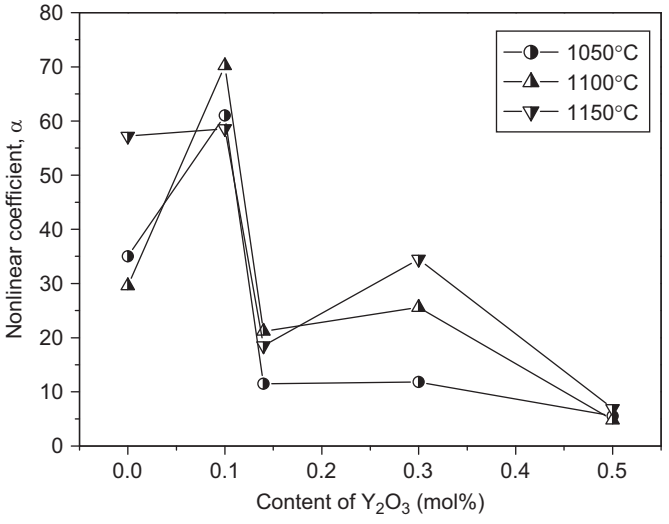

Fig. 7. Variation of nonlinear coefficient α with various contents of Y_2O_3 doped 0.25 mol% Nd_2O_3 added ZnO based varistors sintered at different temperatures.

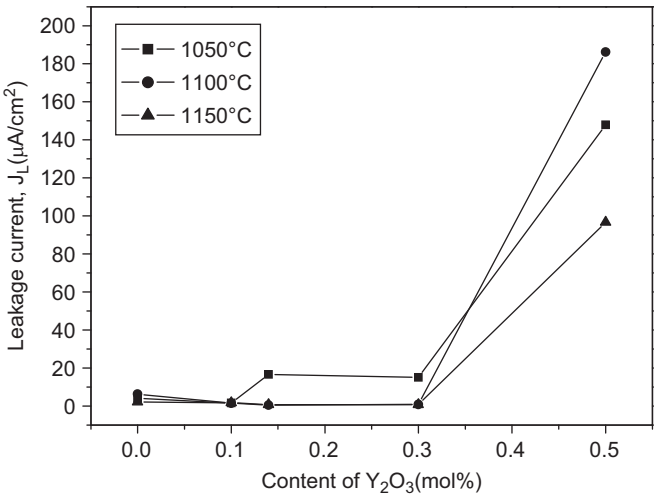

Fig. 8. Leakage current (J_L) of the 0.25 mol% Nd_2O_3 added ZnO based varistor as a function of Y_2O_3 content sintered at different temperatures.

nonlinear coefficient characterizing nonlinearity of a varistor is derived from the *E–J* curves shown in Fig. 5. It is believed that doping appropriate Nd_2O_3 and Y_2O_3 content in ZnO-based varistor ceramics can markedly enhance nonlinearity characteristics. This is involved in the formation of interfacial states and deep bulk traps, both of which contribute to the highly nonlinear properties [21]. However, the sintering temperature has an indefinite effect on the nonlinear coefficient.

Fig. 8 depicts the variation of the leakage current (J_L) with various contents of Y_2O_3 in the 0.25 mol% Nd_2O_3 doped-ZnO based varistor ceramics sintered at different temperatures. It can be found that all samples have low value of leakage current when the content of Y_2O_3 is ≤ 0.3 mol%. However, excess doping Y_2O_3 (>0.3 mol%) significantly results in the increase of leakage current, which may be due to the increase of inter-granular porosity which leads to larger leakage current. On the other hand, the leakage current is also affected by sintering temperature in the range of 1050–1150 °C, as shown in Fig. 8. Typically, the ceramic sample doped with 0.25 mol% Nd_2O_3 and 0.10 mol% Y_2O_3 sintered at 1100 °C has good varistor properties of $J_L = 1.51$ μA/cm^2, $\alpha = 70.2$, and $E = 406$ V/mm.

4. Conclusions

The microstructure and electrical properties of ZnO-based varistor ceramics doped with Nd_2O_3 and different Y_2O_3 contents have been investigated. The XRD and EDS analyses of the samples show presence of primary phase ZnO, and Bi_2O_3, $Zn_7Sb_2O_{12}$, Y_2O_3, Nd-rich phase as well as Y-containing Bi-rich phase as minor secondary phases. The results show that the threshold voltage of the samples co-doped with Nd_2O_3 and Y_2O_3 is higher than the only Nd_2O_3 doped sample. The average size of ZnO grain is found to decrease with the increase of Y_2O_3 content. It can be seen that the nonlinear coefficient initially increases and

then decreases with the increase of Y_2O_3 content. When the content of Y_2O_3 is 0.1 mol%, a big nonlinear coefficient of ZnO-based varistor ceramics can be obtained. It is believed that doping appropriate contents of Nd_2O_3 and Y_2O_3 can markedly enhance nonlinearity characteristics of ZnO-based varistor ceramics. All samples have low value of leakage current when the content of Y_2O_3 is ≤ 0.3 mol%. The varistor ceramics added with 0.25 mol% Nd_2O_3 and 0.10 mol% Y_2O_3 sintered at 1050 °C exhibits excellent electrical properties with the threshold voltage of 556.4 V/mm, the nonlinear coefficient of 61 and the leakage current of 1.55 $\mu A/cm^2$. The results confirm that doping Nd_2O_3 and Y_2O_3 is a very promising route for the production of the higher nonlinear coefficient and the higher threshold voltage ZnO-based varistor ceramics, and determining the proper amounts of addition of Y_2O_3 is of great importance.

References

[1] D.R. Clarke, Varistor ceramics, Journal of the American Ceramic Society 82 (3) (1999) 485–502.

[2] M.A. Ashraf, A.H. Bhuiyan, M.A. Hakim, M.T. Hossain, Microstructure and electrical properties of Sm_2O_3 doped Bi_2O_3 based ZnO varistor ceramics, Materials Science and Engineering B 176 (11) (2011) 855–860.

[3] C.W. Nahm, Microstructure and electrical properties of Dy_2O_3-doped ZnO–Pr_6O_{11} based varistor ceramics, Materials Letters 58 (17–18) (2004) 2252–2255.

[4] M. Houabes, R. Metz, Rare earth oxides effects on both the threshold voltage and energy absorption capability of ZnO varistors, Ceramics International 33 (7) (2007) 1191–1197.

[5] H.Y. Liu, H. Kong, D.M. Jiang, W.Z. Shi, X.X. Ma, Microstructure and electrical properties of Er_2O_3-doped ZnO-based varistor ceramics prepared by high-energy ball milling, Journal of Rare Earths 25 (1) (2007) 120–123.

[6] D. Xu, X.N. Cheng, G.P. Zhao, J. Yang, L.Y. Shi, Microstructure and electrical properties of Sc_2O_3-doped ZnO–Bi_2O_3 based varistor ceramics, Ceramics International 37 (3) (2011) 701–706.

[7] S. Bernik, S. Macek, B. Ai., Microstructural and electrical characteristics of Y_2O_3-doped ZnO–Bi_2O_3 based varistor ceramics, Journal of the European Ceramic Society 21 (10–11) (2001) 1875–1878.

[8] C.W. Nahm, C.H. Park, Effect of Er_2O_3 addition on the microstructure, electrical properties, and stability of Pr_6O_{11}-based ZnO ceramic varistors, Journal of Materials Science 36 (7) (2001) 1671–1679.

[9] C.W. Nahm, Microstructure and electrical properties of Y_2O_3-doped ZnO–Pr_6O_{11}-based varistor ceramics, Materials Letters 57 (7) (2003) 1317–1321.

[10] C.W. Nahm, Effect of La_2O_3 addition on microstructure and electrical properties of ZnO–Pr_6O_{11}-based varistor ceramics, Journal of Materials Science: Materials in Electronics 16 (6) (2005) 345–349.

[11] C.W. Nahm, C.H. Park, H.S. Yoon, Microstructure and varistor properties of ZnO–Pr_6O_{11}–CoO–Nd_2O_3 based ceramics, Journal of Materials Science Letters 19 (4) (2000) 271–274.

[12] M.H. Wang, Q.H. Tang, C. Yao, Electrical properties and AC degradation characteristics of low voltage ZnO varistors doped with Nd_2O_3, Ceramics International 36 (3) (2010) 1095–1099.

[13] Q. Yan, J.Z. Chen, M.J. Tu, Influence of Nd_2O_3 on voltage and microstructure of ZnO varistor materials, Rare Metal Materials and Engineering 34 (1) (2005) 154–157.

[14] S. Bernik, S. Macek, B. Ai, The characteristics of ZnO–Bi_2O_3-based varistor ceramics doped with Y_2O_3 and varying amounts of Sb_2O_3, Journal of the European Ceramic Society 24 (6) (2004) 1195–1198.

[15] C.W. Nahm, The effect of sintering temperature on varistor properties of (Pr, Co, Cr, Y, Al)-doped ZnO ceramics, Materials Letters 62 (29) (2008) 4440–4442.

[16] D. Xu, L.Y. Shi, Z.H. Wu, Q.D. Zhong, X.X. Wu, Microstructure and electrical properties of ZnO–Bi_2O_3-based varistor ceramics by different sintering processes, Journal of the European Ceramic Society 29 (9) (2009) 1789–1794.

[17] D. Xu, X.F. Shi, X.N. Cheng, J. Yang, Y.E. Fan, H.M. Yuan, L.Y. Shi, Microstructure and electrical properties of Lu_2O_3-doped ZnO–Bi_2O_3-based varistor ceramics, Transactions of the Nonferrous Metals Society of China 20 (12) (2010) 2303–2308.

[18] D. Xu, X.N. Cheng, G.P. Zhao, H.X. Xu, Y.E. Fan, L.Y. Shi, Novel mixed rare earths doped ZnO–Bi_2O_3 based varistor ceramics, Journal of University of Science and Technology Beijing 32 (10) (2010) 1316–1320.

[19] D. Xu, X.N. Cheng, H.M. Yuan, J. Yang, Y.H. Lin, Microstructure and electrical properties of Y $(NO_3)_3 \cdot 6H_2O$-doped ZnO–Bi_2O_3-based varistor ceramics, Journal of Alloys and Compounds 509 (38) (2011) 9312–9317.

[20] C.W. Nahm, Effect of MnO_2 addition on microstructure and electrical properties of ZnO–V_2O_5-based varistor ceramics, Ceramics International 35 (2) (2009) 541–546.

[21] M.A. Ashraf, A.H. Bhuiyan, M.A. Hakim, M.T. Hossain, Microstructure and electrical properties of Ho_2O_3 doped Bi_2O_3-based ZnO varistor ceramics, Physica B 405 (17) (2010) 3770–3774.